



HAL
open science

Bottom Mixing Enhanced by Tropical Storm-Generated Near-Inertial Waves Entering Critical Layers in the Straits of Florida

Lixin Qu, Leif Thomas, Jonathan Gula

► **To cite this version:**

Lixin Qu, Leif Thomas, Jonathan Gula. Bottom Mixing Enhanced by Tropical Storm-Generated Near-Inertial Waves Entering Critical Layers in the Straits of Florida. *Geophysical Research Letters*, 2021, 48, 10.1029/2021GL093773 . insu-03683260

HAL Id: insu-03683260

<https://insu.hal.science/insu-03683260>

Submitted on 31 May 2022

HAL is a multi-disciplinary open access archive for the deposit and dissemination of scientific research documents, whether they are published or not. The documents may come from teaching and research institutions in France or abroad, or from public or private research centers.

L'archive ouverte pluridisciplinaire **HAL**, est destinée au dépôt et à la diffusion de documents scientifiques de niveau recherche, publiés ou non, émanant des établissements d'enseignement et de recherche français ou étrangers, des laboratoires publics ou privés.

Copyright

Geophysical Research Letters

RESEARCH LETTER

10.1029/2021GL093773

Key Points:

- A slantwise critical layer for near-inertial waves is observed over the western slope of the Straits of Florida
- Signatures of near-inertial waves are observed in the slantwise critical layer after tropical storms pass over the Straits of Florida
- Upon entering the slantwise critical layer, the waves are trapped and hence amplified, leading to mixing enhancement over the western slope

Supporting Information:

Supporting Information may be found in the online version of this article.

Correspondence to:

L. Qu,
lixinqu@stanford.edu

Citation:

Qu, L., Thomas, L., & Gula, J. (2021). Bottom mixing enhanced by tropical storm-generated near-inertial waves entering critical layers in the Straits of Florida. *Geophysical Research Letters*, *48*, e2021GL093773. <https://doi.org/10.1029/2021GL093773>

Received 7 APR 2021
 Accepted 16 JUL 2021

Bottom Mixing Enhanced by Tropical Storm-Generated Near-Inertial Waves Entering Critical Layers in the Straits of Florida

Lixin Qu¹ , Leif Thomas¹ , and Jonathan Gula^{2,3} 

¹Department of Earth System Science, Stanford University, Stanford, CA, USA, ²Université de Bretagne Occidentale, CNRS, IRD, Ifremer, Laboratoire d'Océanographie Physique et Spatiale, IUEM, Brest, France, ³Institut Universitaire de France (IUF), Paris, France

Abstract Tropical storms and hurricanes frequently pass over the Straits of Florida, energizing the near-inertial wave (NIW) field in the strait. Two ship-based surveys, which were launched shortly after storms, observed velocity shear bands over the western slope of the strait—clear signatures of NIWs. Also, the hydrographic measurements demonstrate the formation of a slantwise critical layer (where isopycnals are parallel with bathymetry) over the western slope, which is known to be a trapping zone for NIWs. A realistic simulation of the Straits confirms the emergence of NIWs under a tropical storm, which is accompanied by inertially modulated bottom-enhanced mixing over the western slope. The mechanism driving the mixing is that the storm-generated NIWs radiate downward from the core of the Florida Current, reflect off the eastern slope, and enter the slantwise critical layer over the western slope; upon entering, wave trapping, and amplification lead to the enhanced mixing.

Plain Language Summary Strong winds blowing over the ocean inject a significant amount of energy into the ocean. Some of this energy goes into near-inertial waves, internal waves radiating from the surface that transmit energy into the ocean interior. Near-inertial waves (NIWs) are thought to play a role in mixing deep waters and sustaining the global overturning circulation. However, they have not been considered as a key driver of mixing near the seafloor. In this study, we present observations of storm-generated NIWs over the seafloor of the Straits of Florida by two research cruises launched shortly after tropical storms. Supported by theories, our numerical simulations show supportive evidence that the seafloor mixing in the Straits of Florida can be enhanced by these storm-generated NIWs. The benthic deep-water coral ecosystems and the properties of intermediate water masses are potentially influenced by this mixing enhancement.

1. Introduction

Enhanced mixing over sloping bathymetry plays an important role in closing global ocean energy budgets and influences deep-water mass transformation and diapycnal upwelling, yielding significant implications for salinity, heat, and nutrient budgets in the abyssal ocean (Callies & Ferrari, 2018; Ferrari et al., 2016; McDougall & Ferrari, 2017; Wunsch & Ferrari, 2004). The bottom-enhanced mixing is highly localized, and one important process driving it is critical reflection of internal waves (Kunze & Smith, 2004), which occurs when the wave's ray slope is close to the bottom slope. Under such circumstances, the focusing of the wave energy would lead to wave amplification and hence wave breaking and enhanced mixing (Cacchione & Wunsch, 1974; Chalamalla et al., 2013). Observations over continental slopes have indicated that internal tides are the major agents undergoing critical reflection and inducing bottom-enhanced mixing as many continental slopes are nearly critical for semidiurnal tidal periods (Gregg et al., 2012; Moum et al., 2002; Nash et al., 2007).

Near-inertial waves (NIWs)—inertia-gravity waves with a frequency near the inertial frequency—carry a significant fraction of the kinetic energy in the internal wave field and are thought to contribute to ocean interior mixing. However, they have not received much attention in terms of critical reflection off sloping bathymetry (Alford et al., 2016). The lack of attention is mainly due to the conception that NIWs propagate nearly horizontally and that, when such waves encounter a steep slope, the waves would be reflected offshore rather than experiencing critical reflection (Cacchione et al., 2002; Kunze & Smith, 2004). However,

theories suggest that the baroclinicity of an oceanic front can significantly steepen the propagation pathways of NIWs, opening the possibility of the critical reflection of NIWs on sloping bottom (Mooers, 1975; Thomas, 2017; Whitt & Thomas, 2013). Qu et al. (2021) demonstrate such a scenario—the so-called slantwise critical layer which can form when isopycnals run parallel to sloping bathymetry. Upon entering this stratified layer, the wave's ray slope approaches the bottom slope with the alignment between the velocity shear bands and the sloping bathymetry, and, more importantly, the group velocity of the waves decreases to zero. Consequently, the wave amplification through trapping leads to turbulence and mixing in this stratified layer over the sloping bottom.

An example of a flow that satisfies the conditions for a slantwise critical layer is the benthic front that blankets the western slope of the Straits of Florida. A turbulent stratified boundary layer is observed within the benthic front with an averaged diffusivity of $4.2 \times 10^{-4} \text{ m}^2/\text{s}$, which is one order of magnitude larger than the ambient water (Winkel et al., 2002). Using the scalings of Gregg (1989) and Polzin et al. (1995), Gregg et al. (1999) and Winkel et al. (2002) attributed the elevated mixing to turbulence associated with the mean shear of the Florida Current and internal wave-wave interaction but they did not consider the trapping of NIWs in slantwise critical layers.

The Straits of Florida is heavily influenced by tropical storms, which input a significant amount of energy into the NIW field. In this article, we will demonstrate, using a combination of numerical simulations and analyses of observations, that the trapping of storm-generated NIWs in slantwise critical layers can elevate mixing in the turbulent stratified boundary layer in the Straits.

2. Observations

A routine survey has been conducted at 27°N in the Straits of Florida to monitor the Florida Current transport since 2001 (Figure 1a) as part of the Western Boundary Time Series project (Meinen et al., 2010; Szuts & Meinen, 2013). The data collected during the surveys include hydrography from conductivity-temperature-depth (CTD) casts, and velocity measurements made using lowered acoustic Doppler current profilers (ADCPs) and shipboard ADCPs (Garcia & Meinen, 2014). The CTD measurements were made at a resolution of 1 m at nine discrete stations (see Figure 1). During the CTD casts, the velocity measurements were made with a 300 kHz lowered ADCP at a resolution of 10 m. More continuous velocity fields across the strait were mapped at a resolution of 10 m in the vertical using a 75 kHz shipboard ADCP which has a maximum profiling range up to 700 m. In this article, we use data collected by 75 cruises from 2001 to 2019, with 3–4 cruises per year.

Two out of the 75 cruises were conducted shortly (2–3 days) after large tropical storms passed the strait—one following Tropical Storm Gordon in September 2018, and the other following Tropical Storm Julia in September 2016 (Figures 1a–1c). Table S1 in the supporting information provides detailed information on the cruises and storms. These timely launches offer a unique opportunity for us to observe storm-generated NIWs. Both cruises observed the slantwise critical layer over the western slope of the strait, where the isopycnals run nearly parallel with the sloping bathymetry (Figures 1d and 1g). Moreover, tilted shear bands were observed over the western slope during both cruises, suggestive of the presence of NIWs (Figures 1f and 1i). The shear bands can be classified into two groups representing two different pathways of NIWs, with one group located at shallower depths (above ~200 m) and the other at deeper depths (below ~300 m). The deeper group of NIWs enters the slantwise critical layer, and the subsequent trapping and amplification of the NIWs should elevate mixing over the western slope according to the theory in Qu et al. (2021).

To identify the pathways of the two groups of NIWs, ray tracing is conducted based on the climatology fields in the strait (see the supporting information for the theory behind the ray-tracing calculation). The climatology includes the potential density and meridional velocity, which are calculated based on the 19-years of cruise data. The climatological potential density suggests that the slantwise critical layer over the western slope is a persistent feature (Figure 1j). The climatological meridional velocity indicates that the vorticity at the surface changes sign in the core of the Florida Current (Figure 1k), where the vorticity gradient is likely maximum and hence a location for the downward radiation of NIWs (see Section 4.1). Another radiation location is at the eastern edge of the strait, where the vorticity gradient is also large (see Figure S1 in the supporting information). Wave rays are initiated at these locations and traced until they reach the separatrix,

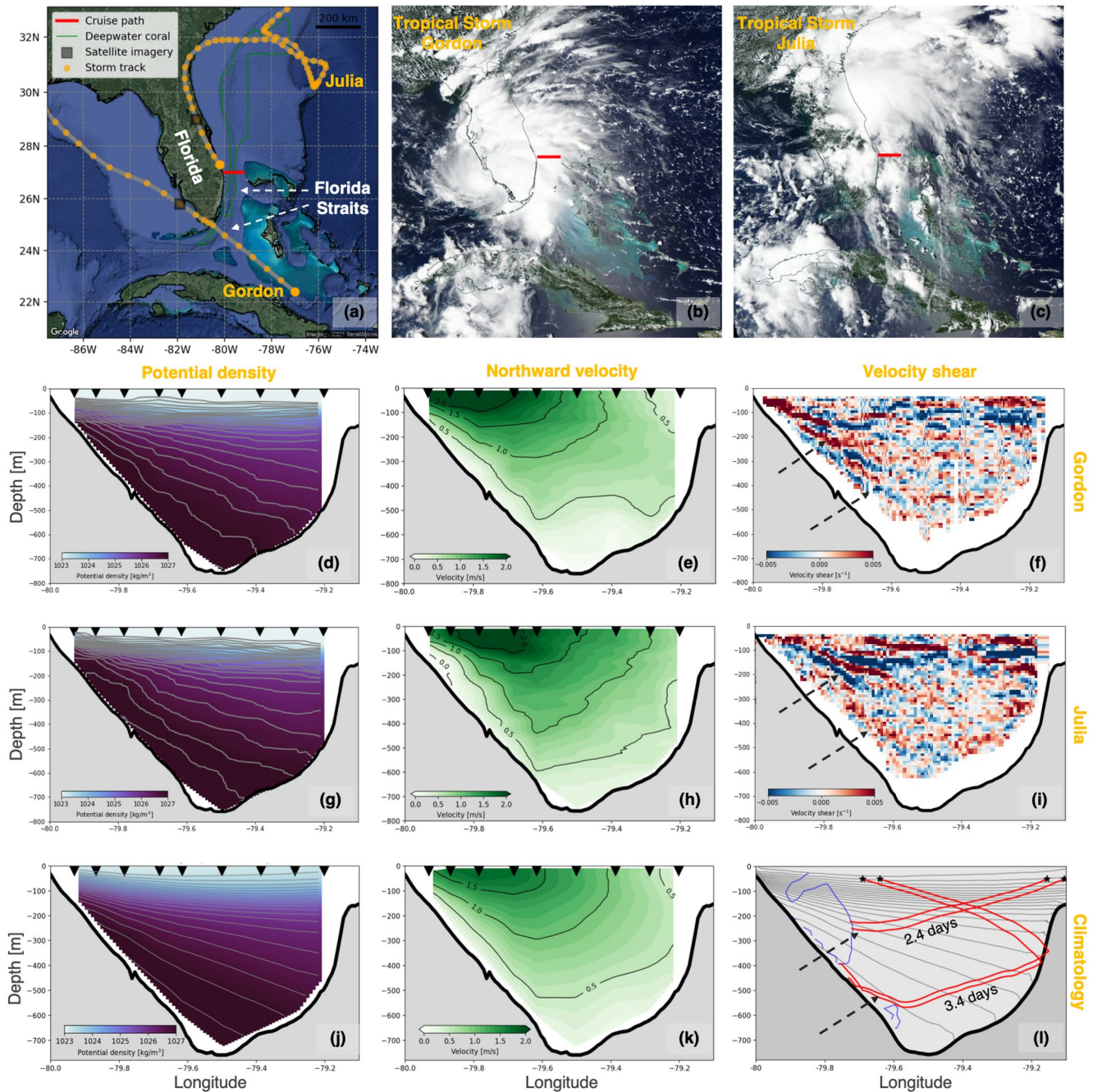


Figure 1. (a) Storm tracks and the cruise path in the Straits of Florida. The storm tracks are from the International Best Track Archive for Climate Stewardship (IBTrACS, Knapp et al., 2010). (b and c) MODIS-AQUA visible images of Storms Gordon and Julia over the strait. The cruise path is marked by the red lines. (d–i) Potential density, meridional velocity, and vertical shear of zonal velocity from the cruises during Storms Gordon and Julia. The triangles denote the sampling stations. (j and k) Climatological averages of potential density and meridional velocity based on the cruises from 2001 to 2019. (l) Ray-tracing solutions. The black stars denote the initial locations of the waves, and the red rays are the pathways of the wave packets. The wave frequency is set to $1.1f_{Lat=27^{\circ}N}$ (equivalent to a period of 24 h). The blue contours mark the separatrix where $\omega_{min} = 1.1f$. The rays and the propagation time are estimated using the extrapolated field of the climatological potential density (contoured) and based on the ray-tracing theory (see the supporting information for details). Isopycnals in (d, g, j, and l) are contoured in gray every 0.2 kg/m^3 .

beyond which the waves become evanescent. As illustrated in Figure 1, we envision that the shallower NIWs originate from the eastern side of the strait, while the deeper NIWs radiate from the Florida Current, reflect off the eastern slope, enter the slantwise critical layer, and enhance mixing over the western slope.

3. Realistic Simulation

Unfortunately, the surveys did not make fine-scale measurements of turbulence, and hence accurate mixing information cannot be directly acquired. Moreover, information on temporal variations was not provided since each survey samples the whole strait only once each time. In lieu of such observations, we use a realistic simulation that is capable of reproducing the responses of the NIWs and associated mixing enhancement under tropical storms to explore the physics of NIWs in the Strait.

The realistic simulation is extracted from a submesoscale-permitting Atlantic wide simulation (GIGATL1) performed with the Coastal and Regional Ocean Community model (CROCO), which is built upon the Regional Oceanic Modeling System (Shchepetkin & McWilliams, 2005, ROMS). It solves the free surface, hydrostatic, and primitive equations using terrain-following vertical coordinates. The simulation domain covers the full Atlantic Ocean with a horizontal resolution that varies between 700 m and 1 km and with 100 vertical levels. The simulation is run from June 2007 to June 2009. Boundary conditions are supplied by the Simple Ocean Data Assimilation (Carton & Giese, 2008, SODA). Initial conditions are provided by a lower resolution version ($dx = 3$ km) of an otherwise identical configuration initialized in January 2004 using SODA as initial and boundary conditions. The simulation is forced by hourly atmospheric forcings from the Climate Forecast System Reanalysis (Saha et al., 2010, CFSR) and includes barotropic tidal forcing at the boundaries and tidal potential and self attraction that are taken, respectively, from TPXO7.2 and GOT99.2b. The bathymetry is taken from the SRTM30plus data set (Becker et al., 2009). The $k - \epsilon$ turbulence closure scheme is used to parameterize vertical mixing, and the Canuto A stability function formulation is applied (Canuto et al., 2001; Umlauf & Burchard, 2003). There is no explicit lateral diffusivity in the simulation. The effect of bottom friction is parameterized through a logarithmic law of the wall with a roughness length $Z_0 = 0.01$ m.

Here, we present the responses of the NIWs and associated mixing enhancement during Tropical Storm Fay, which moved over the strait in mid-August, 2008 (Figure 2a). At 27°N the winds start to increase at 19:00 on August 17th and maintain a speed exceeding 10 m/s for about 3 days (Figure 2b). Noticing that the inertial period at 27°N is 26.4 h, the turbulent shear production $P \equiv -\overline{u'w'} \frac{\partial u}{\partial z} - \overline{v'w'} \frac{\partial v}{\partial z}$ over the western slope exhibits a near-inertial pulsing about 3 days after the wind burst (Figure 2c). The enhancement of P indicates the enhancement of mixing, because P is the direct energy supply for the turbulent kinetic energy (TKE) dissipation rate ϵ and the turbulent buoyancy flux $B \equiv \overline{b'w'}$ based on the $k - \epsilon$ model (Warner et al., 2005). The near-inertial variability of P suggests that the enhanced mixing is related to NIWs. As illustrated in Figures 2d and 2a slantwise critical layer is formed over the western slope, and the ray-tracing solution suggests that the NIWs radiating from the Florida Current could enter the slantwise critical layer. This pathway of NIWs is indeed reflected in the field of vertical shear with the shear bands largely paralleling the wave rays (Figure 2f). Correspondingly, the mixing enhancement blankets the deep western strait (from 300 to 700 m roughly) over a thickness of about 30 m. This region with the enhanced mixing coincides with the turbulent stratified boundary layers, that were identified by Winkel et al. (2002) using microstructure measurements at 27°N in the strait. We explore the underlying mechanism driving the enhanced mixing within the stratified boundary layers over the western slope in the next section. The mixing over the eastern slope of the Straits is also near-inertially enhanced during the storm due to critical reflection of NIWs (see the supporting information for the detail).

4. Mechanism Driving the Mixing Enhancement

4.1. Conceptual Model

A simple 2D conceptual model is developed to illustrate the mechanism driving the mixing enhancement over the western slope of the strait (see the schematic in Figure 3). The model consists of three key elements: (a) radiation of NIWs out of the core of the Florida Current; (b) downward reflection of NIWs off

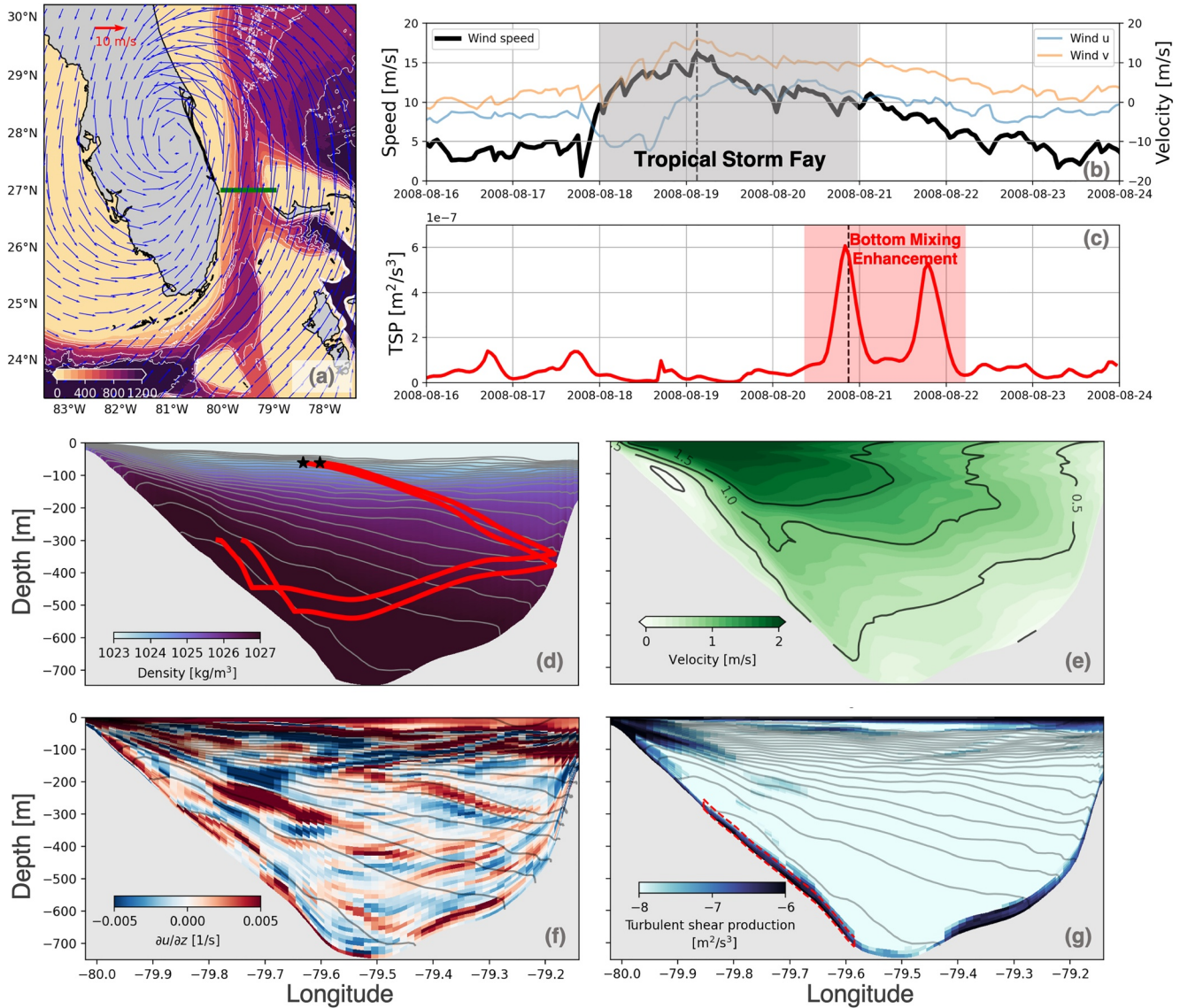


Figure 2. Results of the realistic simulation. (a) Surface winds (vectors) of Tropical Storm Fay from Climate Forecast System Reanalysis/NOAA and the strait bathymetry (color) from SRTM30plus. The snapshot of the winds is made at 03:00 on August 19, 2008, which is denoted in (b) by the dashed line. (b) Time series of the zonal (blue), meridional (yellow) components, and speed of the winds during the storm. The properties are averaged across the strait along 27°N (along the green line in (a)). (c) Time series of the turbulent shear production, $P \equiv -\overline{u'w'} \frac{\partial u}{\partial z} - \overline{v'w'} \frac{\partial v}{\partial z} = \nu \left[\left(\frac{\partial u}{\partial z} \right)^2 + \left(\frac{\partial v}{\partial z} \right)^2 \right]$, where ν is the viscosity. P is averaged within the control volume denoted in (g) by the dashed box. (d–g) Across-strait sections of the potential density, meridional velocity, vertical shear of zonal velocity, and turbulent shear production along 27°N. The red lines in (d) are the wave rays calculated by setting the wave frequency of $1.1f |_{LAI=27^\circ N}$ (equivalent to a period of 24 h). These sections are made at 21:00 on August 20, 2008, which is denoted in (c) by the dashed line. The potential density is contoured every 0.2 kg/m^3 in (d, f, and g).

the eastern slope; (c) trapping of NIWs in the slantwise critical layer over the western slope. Each element is elaborated in more detail below.

The storm inputs energy into near-inertial motions and energizes a NIW field with large horizontal scales near the surface. However, to radiate downwards, NIWs need to reduce their wavelength to increase their vertical group velocity. Via a mechanism known as ζ -refraction, the lateral wavelength of NIWs can be efficiently reduced at locations where gradients in vertical vorticity, ζ , are large, and, as the wavelength shrinks, the NIWs can radiate into the interior (Asselin & Young, 2020; Young & Jelloul, 1997). Based on the

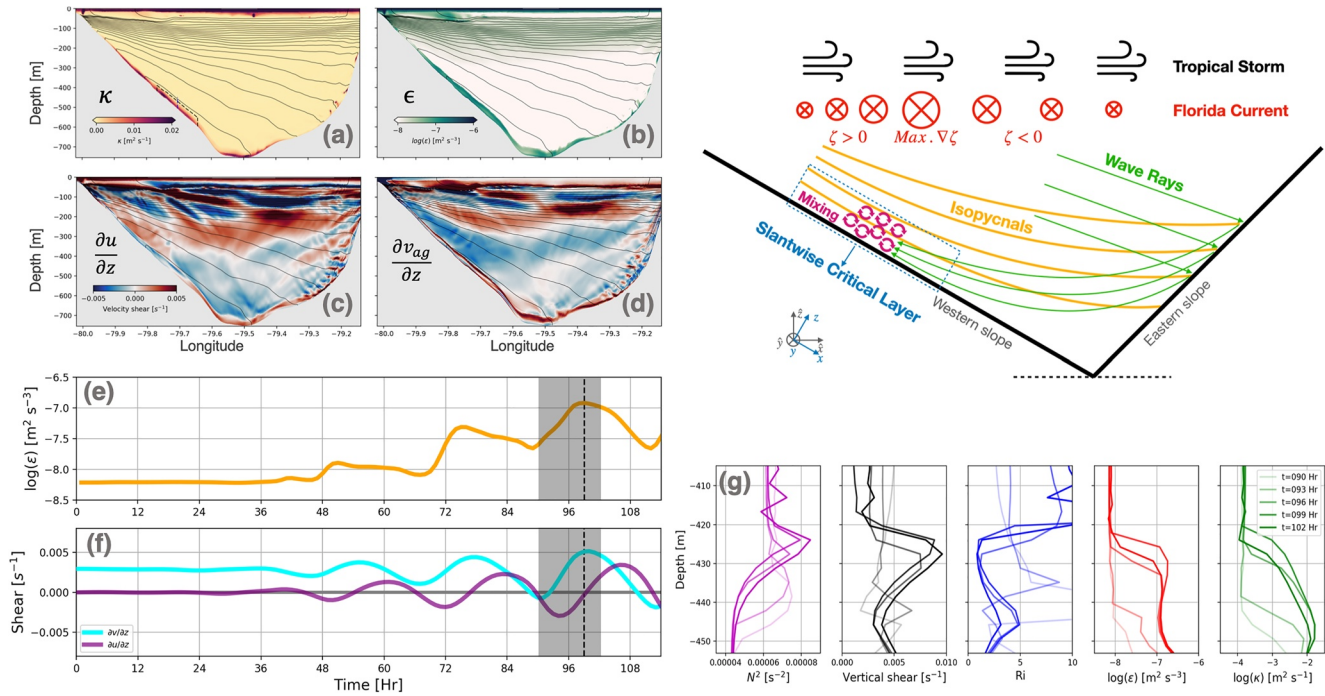


Figure 3. Schematic of the theoretical model and the idealized simulation results. (a–d) Cross-strait sections of diffusivity κ , turbulent kinetic energy dissipation rate ϵ , vertical shear of zonal velocity $\frac{\partial u}{\partial z}$, and vertical shear of ageostrophic meridional velocity $\frac{\partial v_{ag}}{\partial z}$. The sections are made at $t = 99\text{ Hr}$ denoted by the dashed line in (e and f). The potential density is contoured very 0.2 kg/m^3 . (e and f) Time series of ϵ , $\frac{\partial u}{\partial z}$, and $\frac{\partial v}{\partial z}$, which are averaged within the control volume marked by the dashed box in (a). (g) Evolution of stratification, total vertical shear $\sqrt{\left(\frac{\partial u}{\partial z}\right)^2 + \left(\frac{\partial v}{\partial z}\right)^2}$, Richardson number $\frac{N^2}{\sqrt{\left(\frac{\partial u}{\partial z}\right)^2 + \left(\frac{\partial v}{\partial z}\right)^2}}$, ϵ , and κ during the enhancement period shaded in (e and f). The profiles are made at the center of the control volume.

surface velocity profile (Figure S1 in the supporting information), the core of the Florida Current would be such a location where NIWs are preferentially radiated downwards via ζ -refraction.

In the presence of a background current, NIWs can propagate vertically in regions of anti-cyclonic vorticity because of the modification of the effective minimum frequency (Kunze, 1985; Mooers, 1975). To the east of the current core, the vorticity is anti-cyclonic, and hence allows for an eastward and downward propagation pathway of the NIWs. As the NIWs approach and reflect off the eastern slope, not only the vorticity but also the baroclinicity can modify the propagation of the waves, resulting in wave rays with slopes

$$s_{ray} = s_{\rho} \pm \sqrt{\frac{\omega^2 - \omega_{min}^2}{N^2}}, \quad (1)$$

where s_{ρ} is the isopycnal slope, ω is the wave frequency, and $\omega_{min} = f\sqrt{1 + Ro_g - Ri_g^{-1}}$ is the minimum frequency allowable for the waves, $N^2 = \frac{\partial b}{\partial z}$, $Ro_g = \frac{\zeta}{f}$, $Ri_g = \frac{N^2 f^2}{|\nabla_h b|^2}$, b is the buoyancy, and the subscript of

h denotes the horizontal gradient (Thomas, 2017; Whitt & Thomas, 2013). According to Equation 1, the rays of the incident and reflected waves have to be symmetric with respect to isopycnals. As a consequence, the waves are reflected into the deeper strait and propagate westward toward the slantwise critical layer over the western slope.

In the slantwise critical layer, the alignment between the isopycnals and the sloping bottom ensures a background geostrophic flow with $Ro_g = Ri_g^{-1}$, where Ro_g is the Rossby number and Ri_g is the balanced Richardson number (Qu et al., 2021). Consequently, the modifications from the vorticity (encompassed in Ro_g)

and the baroclinicity (encompassed in Ri_g) cancel out with each other such that the minimum frequency allowable for NIWs is precisely inertial, $\omega_{min} = f$. According to Equation 1, $\omega_{min} = f$ ensures $s_{ray} = s_\rho$ for NIWs with $\omega = f$, and hence the associated wave rays are aligned with the sloping bottom in a slantwise critical layer. Moreover, when ω approaches ω_{min} , the group velocity vanishes, leading to wave trapping. So, upon entering the slantwise critical layer, the trapping of the NIWs induce wave amplification and hence enhance the mixing over the western slope of the strait.

4.2. Idealized Simulation

A 2.5D idealized simulation is designed to test the conceptual model, in which the ROMS is employed. The domain is based on the realistic bathymetry of the strait at 27°N in the across-strait direction and set to be invariant in the along-strait direction. The Coriolis parameter is set to $f = f|_{Lat=27^\circ N}$. The simulation is initialized using the climatological fields at 27°N (which are constructed based on the surveys from 2001 to 2019; see Figure S2). The model is forced by an oscillatory wind stress with an amplitude of 0.3 N/m² and a frequency of 1.1 f . See the supporting information for details on the model configuration.

Consistent with the realistic simulation, the idealized simulation also shows that the mixing over the western slope is enhanced with an elevated TKE dissipation rate ϵ and diffusivity κ (Figures 3a and 3b). The pattern of the vertical shear indicates that the NIWs radiate out of the core of the Florida Current, reflect off the eastern slope, and enter the slantwise critical layer over the western slope. The propagation pathway is similar to that in the survey observations and the realistic simulation (Figures 3c and 3d). The averaged ϵ over the western slope exhibits near-inertial pulsing about 3 days after the wind forcing is turned on, which is consistent with the realistic simulation (Figure 3e). The near-inertial pulsing of ϵ is suggestive of a causal link with the NIWs.

Upon entering the slantwise critical layer, the NIWs get trapped, leading to accumulation of wave energy and hence enhanced vertical shear. The idealized simulation shows that the vertical shear in the slantwise critical layer is significantly elevated 2–3 days after the wind forcing is turned on (Figure 3f). Moreover, noting that the background shear is positive (see the early stage in Figure 3f), $\frac{\partial v}{\partial z}$ reaches a maximum when the wave shear aligns with the background shear. As a consequence, this shear alignment phases the mixing enhancement. For instance, the evolution during the mixing enhancement from 90 to 102 Hr shows that, as the total shear is elevated due to the shear alignment, the Richardson number is significantly reduced, resulting in the enhanced mixing in the stratified layer that is evidenced by the elevated ϵ and κ (Figure 3g).

In contrast to the coastal slantwise critical layers in the northern Gulf of Mexico (Qu et al., 2021), the slantwise critical layer in the Straits of Florida is deep, the vertical shear in the background flow is strong, and the NIWs entering the layer are relatively weak with an amplitude one order of magnitude smaller. This leads to a difference in the mechanisms controlling the near-inertial pulsing of mixing. In the case of the northern Gulf of Mexico, the strong NIWs significantly modify the background density field and drive an asymmetric oscillation in the across-shore pressure gradient force with stronger amplitudes at the phases with onshore currents in the slantwise critical layer (Qu et al., 2021). Consequently, the convergence of the wave energy flux pulses at certain phases of the NIWs (i.e., the phases with onshore currents), resulting in a near-inertial pulsing in the bottom mixing. In the case of the Straits of Florida, the NIWs are in a weak and linear regime, and the near-inertial pulsing of mixing is driven by the shear alignment that occurs near-inertially. Nevertheless, both mixing enhancements are due to wave trapping in the slantwise critical layers.

5. Discussion

Sixty tropical storms/hurricanes passed the Straits of Florida from 2001 to 2020 (see Figure 4a for the storm tracks), indicating a significant amount of energy input into the NIW field. However, NIWs form not only during tropical storms/hurricanes but also in other strong-wind events that are not induced by tropical storms/hurricanes. Consequently, enhancement of mixing in the deep strait can also be driven during the nonstorm wind events via NIW trapping. Here, we discuss the relative importance of tropical storms/hurricanes in generating NIWs in the Straits versus other strong-wind events. The wind events over the Straits are recognized if the wind speed is over 10 m/s and are classified as either storm events or strong-wind events

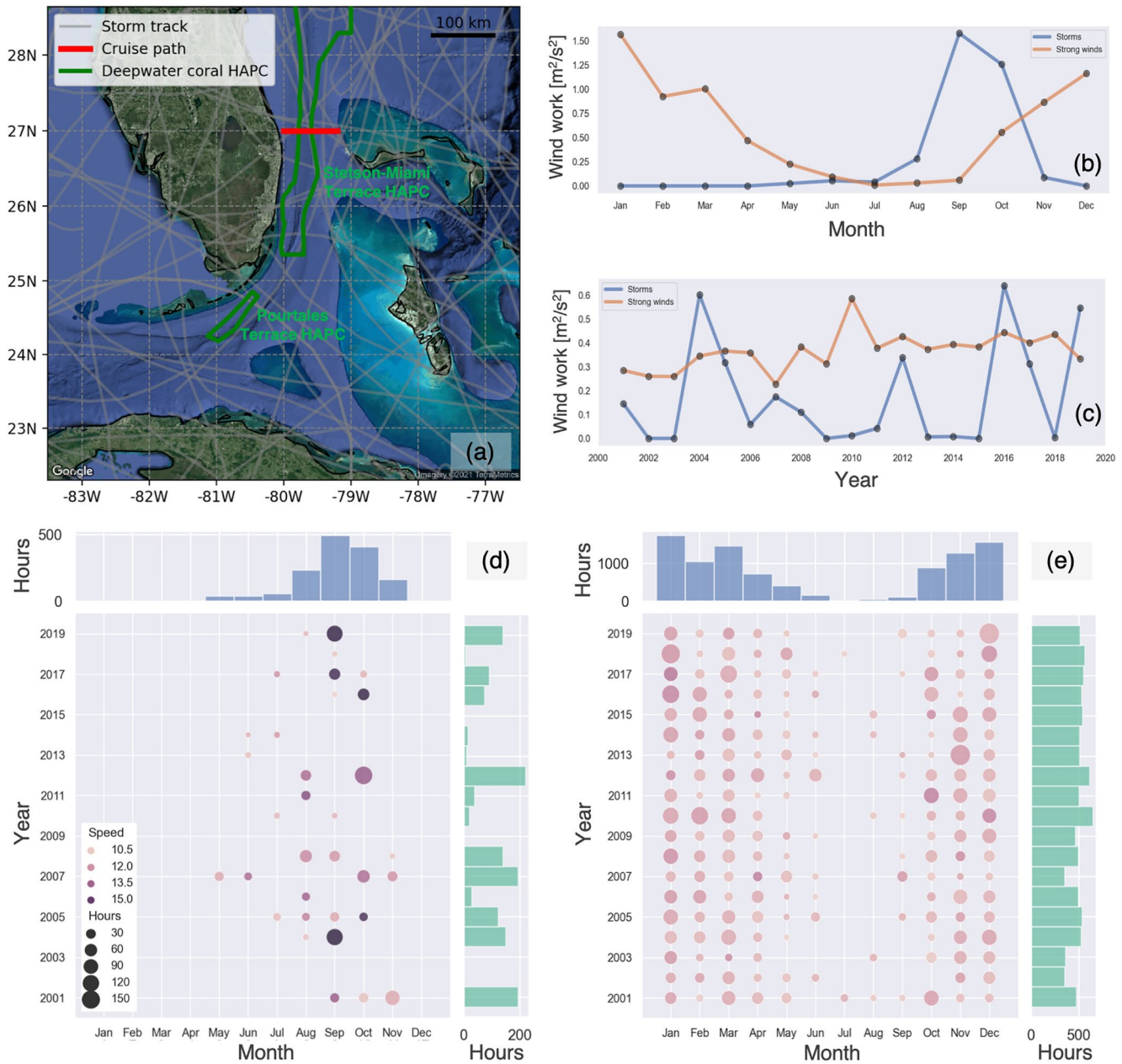


Figure 4. (a) The Storm tracks (gray lines) from 2001 to 2020 and the deep-water coral habitat areas of particular concern (HAPCs; green polygons). The storm tracks are from International Best Track Archive for Climate Stewardship. (b and c) Wind work $WORK_{TS}$ (blue) and $WORK_{SW}$ (yellow) as functions of month and year. (d) Scatter plot of the wind events related to the tropical storms/hurricanes from 2001 to 2009. The color denotes the wind speed in units of m/s, and the size denotes the duration in units of hours. Histograms of the duration are attached at the axes. (e) Same as (d) but for the nonstorm wind events. The winds are averaged between $-80^{\circ}W$ and $-79^{\circ}W$ and along $27^{\circ}N$ using the Climate Forecast System Reanalysis data set.

depending on whether a storm passed by the strait. Figures 4d and 4e show the statistics of these two groups of wind events in terms of strength and persistence. The storm events tend to occur in summer and fall, exhibiting short and intermittent characteristics combined with strong bursts, while the strong-wind events often occur in winter, exhibiting long and regulated persistence with mildly strong winds.

To understand the relative importance of these two groups of winds on energizing NIWs, the wind work of each group is estimated via a slab mixed layer model as follows:

$$\frac{\partial u_{ML}}{\partial t} - f v_{ML} = \frac{\tau_x}{\rho_0 H_{ML}} - r u_{ML}, \quad (2)$$

$$\frac{\partial v_{ML}}{\partial t} + f u_{ML} = \frac{\tau_y}{\rho_0 H_{ML}} - r v_{ML}, \quad (3)$$

where (u_{ML}, v_{ML}) are the mixed layer velocities, $f = f_{27^\circ N}$ is the Coriolis parameter, (τ_x, τ_y) is the wind stress, $\rho_0 = 1025 \text{ kg/m}^3$ is the reference density, $H_{ML} = 50 \text{ m}$ is the mixed layer thickness, and $r = \frac{1}{2} f$ is the damping coefficient (Pollard & Millard, 1970). The solutions of the slab mixed layer model are not sensitive to the magnitude of r and do not qualitatively change if the coefficient is in the range $1/r = 0.1 - 1$ days (D'Asaro, 1985; Whitt & Thomas, 2015). The wind stress is calculated based on a quadratic equation, $\vec{\tau} = C_d \rho_{air} |\vec{U}_{10}| \vec{U}_{10}$, where $C_d = 1.5 \times 10^{-3}$ is the drag coefficient, $\rho_{air} = 1.225 \text{ kg/m}^3$ is the air density, and \vec{U}_{10} is the wind velocity 10 m above the sea (Cushman-Roisin & Beckers, 2011). The wind velocity is extracted from the CFSR/NOAA data set and averaged between $-80^\circ W$ and $-79^\circ W$ and along $27^\circ N$.

Forced by the wind stress, the slab mixed layer model is integrated to yield the mixed layer velocities so that the wind work can be estimated. By definition, the wind work integrated through a certain period T as follows:

$$WORK = \int_T \frac{\tau_x u_{ML} + \tau_y v_{ML}}{\rho_0 H_{ML}} dt. \quad (4)$$

The wind work represents the energy input into the NIW field by the winds and yields an upper bound on the wave energy flux into the ocean interior. The wind work is attributed to the two groups by integrating through two different periods. The period for the tropical storms/hurricanes T_{TS} is defined by when the wind speed is over 10 m/s and a storm passes over, while the period for the strong-wind events T_{SW} is when the wind speed surpasses the same cutoff but the high speed is not driven by any tropical storms/hurricanes. The wind work $WORK_{TS}$ and $WORK_{SW}$ are then determined by integrating over T_{TS} and T_{SW} , respectively. The statistics show $WORK_{TS}$ and $WORK_{SW}$ as functions of month and year (Figures 4b and 4c). If shown in month (year), the wind work is calculated by integrating Equation 4 over the T_{TS} / T_{SW} of a certain month (year) over all years (months). It is suggested that $WORK_{TS}$ and $WORK_{SW}$ take turns to dominate in different seasons with similar magnitudes, and $WORK_{SW}$ maintains at a stable level with the magnitude comparable to $WORK_{TS}$ of the years with intense storms. Consequently, it could be inferred that the long persistence of the winds makes the strong-wind events an equivalently important contributor to energize the NIWs. Overall, both the tropical storms/hurricanes and strong-wind events input a significant amount of energy into the NIW field and could play equally important roles on driving the enhancement of bottom mixing, yielding potential environmental implications in the deep strait.

The Straits of Florida is a habitat with extensive deep-sea coral ecosystems (Reed et al., 2013). Deep-sea corals provide shelters and host deep-water ecosystems (Wilson et al., 2006). Two deep-water coral habitat areas of particular concern (HAPCs; Figure 4a) are designated between Florida and the Bahamas in the deep western strait (NOAA, 2010), where the mixing could be enhanced by NIWs. The mixing enhancement could alter the levels of temperature, oxygen, and PH that the corals experience and may cause sediment re-suspension that would provide particulate organic matter for the corals, suggesting important implications for the benthic ecosystems.

Another potential impact of the enhanced mixing worth noting is related to Antarctic Intermediate Water (AAIW). Induced by the upslope bottom Ekman transport, AAIW blankets over the western bottom of the strait (Seim et al., 1999). AAIW is a cold, low salinity water mass that distinguishes from the upper warmer, saltier water in the strait which is originated from the subtropical South Atlantic (Atkinson, 1983; Schmitz & Richardson, 1991). The enhanced mixing by NIWs could affect the abyssal diapycnal transport and hence potentially modify the properties of AAIW before it joins the North Atlantic, which could have significant implications for the distribution of biogeochemical tracers downstream.

Data Availability Statement

The CTD and ADCP data used in this study are available online (<https://www.aoml.noaa.gov/phod/wbts/data.php>). The satellite imagery from the MODIS-AQUA are available online through the WORLDVIEW supported by the National Aeronautics and Space Administration (<https://worldview.earthdata.nasa.gov>). The information about the GIGATL1 can be found at <https://doi.org/10.5281/zenodo.4948523>.

Acknowledgments

This work was funded by the SUNRISE project, NSF grant number OCE-1851450 (L. Qu and L. Thomas). J. Gula gratefully acknowledges support from the French National Agency for Research (ANR) through the project DEEPER (ANR-19-CE01-0002-01). The research cruises used in this study were funded by the Western Boundary Time Series project, which is supported by the Climate Program Office of the NOAA. The authors acknowledge PRACE and GENCI for awarding us access to HPC resources Joliot-Curie Rome and SKL from GENCI-TGCC (Grants 2020-A0090112051, 2019gch0401, and PRACE project 2018194735) and HPC facilities DATARMOR of “Pôle de Calcul Intensif pour la Mer” at Ifremer Brest France. The authors thank Gildas Cambon and Sébastien Theetten for their contribution in the development of the realistic numerical simulation GIGATL1. The authors thank Jennifer MacKinnon and Kathryn Shamberger for very helpful suggestions when preparing this manuscript.

References

Alford, M. H., MacKinnon, J. A., Simmons, H. L., & Nash, J. D. (2016). Near-inertial internal gravity waves in the ocean. *Annual Review of Marine Science*, 8, 95–123. <https://doi.org/10.1146/annurev-marine-010814-015746>

Asselin, O., & Young, W. R. (2020). Penetration of wind-generated near-inertial waves into a turbulent ocean. *Journal of Physical Oceanography*, 50(6), 1699–1716. <https://doi.org/10.1175/jpo-d-19-0319.1>

Atkinson, L. P. (1983). Distribution of antarctic intermediate water over the Blake Plateau. *Journal of Geophysical Research*, 88(C8), 4699–4704. <https://doi.org/10.1029/JC088iC08p04699>

Becker, J. J., Sandwell, D. T., Smith, W. H. F., Braud, J., Binder, B., Depner, J., et al. (2009). Global bathymetry and elevation data at 30 arc seconds resolution: SRTM30_PLUS. *Marine Geodesy*, 32(4), 355–371. <https://doi.org/10.1080/01490410903297766>

Cacchione, D., Pratson, L., & Ogston, A. (2002). The shaping of continental slopes by internal tides. *Science*, 296, 724–727. <https://doi.org/10.1126/science.1069803>

Cacchione, D., & Wunsch, C. (1974). Experimental study of internal waves over a slope. *Journal of Fluid Mechanics*, 66, 223–239. <https://doi.org/10.1017/s0022112074000164>

Callies, J., & Ferrari, R. (2018). Dynamics of an abyssal circulation driven by bottom-intensified mixing on slopes. *Journal of Physical Oceanography*, 48, 1257–1282. <https://doi.org/10.1175/jpo-d-17-0125.1>

Canuto, V. M., Howard, A., Cheng, Y., & Dubovikov, M. (2001). Ocean turbulence. Part I: One-point closure model—Momentum and heat vertical diffusivities. *Journal of Physical Oceanography*, 31(6), 1413–1426. [https://doi.org/10.1175/1520-0485\(2001\)031<1413:otpiop>2.0.co;2](https://doi.org/10.1175/1520-0485(2001)031<1413:otpiop>2.0.co;2)

Carton, J., & Giese, B. (2008). A reanalysis of ocean climate using Simple Ocean Data Assimilation (SODA). *Monthly Weather Review*, 136, 2999–3017. <https://doi.org/10.1175/2007mwr1978.1>

Chalamalla, V., Gayen, B., Scotti, A., & Sarkar, S. (2013). Turbulence during the reflection of internal gravity waves at critical and near-critical slopes. *Journal of Fluid Mechanics*, 729, 47–68. <https://doi.org/10.1017/jfm.2013.240>

Cushman-Roisin, B., & Beckers, J.-M. (2011). *Introduction to geophysical fluid dynamics: Physical and numerical aspects*. Academic Press.

D’Asaro, E. A. (1985). The energy flux from the wind to near-inertial motions in the surface mixed layer. *Journal of Physical Oceanography*, 15(8), 1043–1059.

Ferrari, R., Mashayek, A., McDougall, T., Nikurashin, M., & Campin, J. (2016). Turning ocean mixing upside down. *Journal of Physical Oceanography*, 46, 2239–2261. <https://doi.org/10.1175/jpo-d-15-0244.1>

García, R. F., & Meinen, C. S. (2014). Accuracy of Florida Current volume transport measurements at 27 n using multiple observational techniques. *Journal of Atmospheric and Oceanic Technology*, 31(5), 1169–1180. <https://doi.org/10.1175/jtech-d-13-00148.1>

Gregg, M. (1989). Scaling turbulent dissipation in the thermocline. *Journal of Geophysical Research*, 94(C7), 9686–9698. <https://doi.org/10.1029/JC094iC07p09686>

Gregg, M., Alford, M., Kontoyiannis, H., Zervakis, V., & Winkel, D. (2012). Mixing over the steep side of the Cycladic Plateau in the Aegean Sea. *Journal of Marine Systems*, 89(1), 30–47. <https://doi.org/10.1016/j.jmarsys.2011.07.009>

Gregg, M., Winkel, D., MacKinnon, J., & Lien, R. (1999). Mixing over shelves and slopes. In P. Müller, & D. Henderson (Eds.), *Dynamics of oceanic internal gravity waves II, proceedings, Hawaiian winter workshop* (pp. 35–42).

Knapp, K. R., Kruk, M. C., Levinson, D. H., Diamond, H. J., & Neumann, C. J. (2010). The international best track archive for climate stewardship (IBTrACS) unifying tropical cyclone data. *Bulletin of the American Meteorological Society*, 91(3), 363–376. <https://doi.org/10.1175/2009bams2755.1>

Kunze, E. (1985). Near-inertial wave propagation in geostrophic shear. *Journal of Physical Oceanography*, 15(5), 544–565. [https://doi.org/10.1175/1520-0485\(1985\)015<0544:niwpig>2.0.co;2](https://doi.org/10.1175/1520-0485(1985)015<0544:niwpig>2.0.co;2)

Kunze, E., & Smith, S. L. (2004). The role of small-scale topography in turbulent mixing of the global ocean. *Oceanography*, 17(1), 55–64. <https://doi.org/10.5670/oceanog.2004.67>

McDougall, T., & Ferrari, R. (2017). Abyssal upwelling and downwelling driven by near-boundary mixing. *Journal of Physical Oceanography*, 47, 261–283. <https://doi.org/10.1175/jpo-d-16-0082.1>

Meinen, C. S., Baringer, M. O., & Garcia, R. F. (2010). Florida Current transport variability: An analysis of annual and longer-period signals. *Deep Sea Research Part I: Oceanographic Research Papers*, 57(7), 835–846. <https://doi.org/10.1016/j.dsr.2010.04.001>

Mooers, C. N. (1975). Several effects of a baroclinic current on the cross-stream propagation of inertial-internal waves. *Geophysical and Astrophysical Fluid Dynamics*, 6(3), 245–275. <https://doi.org/10.1080/03091927509365797>

Moum, J., Caldwell, D., Nash, J., & Gunderson, G. (2002). Observations of boundary mixing over the continental slope. *Journal of Physical Oceanography*, 32(7), 2113–2130. [https://doi.org/10.1175/1520-0485\(2002\)032<2113:oobmot>2.0.co;2](https://doi.org/10.1175/1520-0485(2002)032<2113:oobmot>2.0.co;2)

Nash, J., Alford, M., Kunze, E., Martini, K., & Kelly, S. (2007). Hotspots of deep ocean mixing on the Oregon continental slope. *Geophysical Research Letters*, 34, L01605. <https://doi.org/10.1029/2006GL028170>

NOAA. (2010). Fisheries of the Caribbean, Gulf of Mexico, and South Atlantic; comprehensive ecosystem-based amendment for the south Atlantic region. *Federal Register*, 75(119), 35330–35335.

Pollard, R. T., & Millard, R., Jr. (1970). Comparison between observed and simulated wind-generated inertial oscillations. *Deep Sea Research and Oceanographic Abstracts*, 17, 813–821. [https://doi.org/10.1016/0011-7471\(70\)90043-4](https://doi.org/10.1016/0011-7471(70)90043-4)

Polzin, K. L., Toole, J. M., & Schmitt, R. W. (1995). Finescale parameterizations of turbulent dissipation. *Journal of Physical Oceanography*, 25(3), 306–328. [https://doi.org/10.1175/1520-0485\(1995\)025<0306:fpotd>2.0.co;2](https://doi.org/10.1175/1520-0485(1995)025<0306:fpotd>2.0.co;2)

Qu, L., Thomas, L. N., & Hetland, R. D. (2021). Near-inertial wave critical layers over sloping bathymetry. *Journal of Physical Oceanography*, 51, 1737–1756. <https://doi.org/10.1175/jpo-d-20-0221.1>

- Reed, J. K., Messing, C., Walker, B. K., Brooke, S., Correa, T. B., Brouwer, M., et al. (2013). Habitat characterization, distribution, and areal extent of deep-sea coral ecosystems off Florida, southeastern USA. *Caribbean Journal of Science*, 47(1), 13–30. <https://doi.org/10.18475/cjos.v47i1.a3>
- Saha, S., Moorthi, S., Pan, H.-L., Wu, X., Wang, J., Nadiga, S., et al. (2010). The NCEP climate forecast system reanalysis. *Bulletin of the American Meteorological Society*, 91(8), 1015–1058. <https://doi.org/10.1175/2010bams3001.1>
- Schmitz, W. J., Jr., & Richardson, P. L. (1991). On the sources of the Florida Current. *Deep Sea Research Part A. Oceanographic Research Papers*, 38, S379–S409. [https://doi.org/10.1016/s0198-0149\(12\)80018-5](https://doi.org/10.1016/s0198-0149(12)80018-5)
- Seim, H. E., Winkel, D. P., Gawarkiewicz, G., & Gregg, M. C. (1999). A benthic front in the Straits of Florida and its relationship to the structure of the Florida Current. *Journal of Physical Oceanography*, 29(12), 3125–3132. [https://doi.org/10.1175/1520-0485\(1999\)029<3125:abfits>2.0.co;2](https://doi.org/10.1175/1520-0485(1999)029<3125:abfits>2.0.co;2)
- Shchepetkin, A. F., & McWilliams, J. C. (2005). The regional oceanic modeling system (ROMS): A split-explicit, free-surface, topography-following-coordinate oceanic model. *Ocean Modelling*, 9(4), 347–404. <https://doi.org/10.1016/j.ocemod.2004.08.002>
- Szuts, Z. B., & Meinen, C. (2013). Salinity transport in the Florida straits. *Journal of Atmospheric and Oceanic Technology*, 30(5), 971–983. <https://doi.org/10.1175/jtech-d-12-00133.1>
- Thomas, L. N. (2017). On the modifications of near-inertial waves at fronts: Implications for energy transfer across scales. *Ocean Dynamics*, 67(10), 1335–1350. <https://doi.org/10.1007/s10236-017-1088-6>
- Umlauf, L., & Burchard, H. (2003). A generic length-scale equation for geophysical turbulence models. *Journal of Marine Research*, 61(2), 235–265. <https://doi.org/10.1357/002224003322005087>
- Warner, J. C., Sherwood, C. R., Arango, H. G., & Signell, R. P. (2005). Performance of four turbulence closure models implemented using a generic length scale method. *Ocean Modelling*, 8(1–2), 81–113. <https://doi.org/10.1016/j.ocemod.2003.12.003>
- Whitt, D. B., & Thomas, L. N. (2013). Near-inertial waves in strongly baroclinic currents. *Journal of Physical Oceanography*, 43(4), 706–725. <https://doi.org/10.1175/jpo-d-12-0132.1>
- Whitt, D. B., & Thomas, L. N. (2015). Resonant generation and energetics of wind-forced near-inertial motions in a geostrophic flow. *Journal of Physical Oceanography*, 45(1), 181–208. <https://doi.org/10.1175/jpo-d-14-0168.1>
- Wilson, S. K., Graham, N. A., Pratchett, M. S., Jones, G. P., & Polunin, N. V. (2006). Multiple disturbances and the global degradation of coral reefs: Are reef fishes at risk or resilient? *Global Change Biology*, 12(11), 2220–2234. <https://doi.org/10.1111/j.1365-2486.2006.01252.x>
- Winkel, D. P., Gregg, M. C., & Sanford, T. B. (2002). Patterns of shear and turbulence across the Florida Current. *Journal of Physical Oceanography*, 32(11), 3269–3285. [https://doi.org/10.1175/1520-0485\(2002\)032<3269:posata>2.0.co;2](https://doi.org/10.1175/1520-0485(2002)032<3269:posata>2.0.co;2)
- Wunsch, C., & Ferrari, R. (2004). Vertical mixing, energy, and the general circulation of the oceans. *Annual Review of Fluid Mechanics*, 36, 281–314. <https://doi.org/10.1146/annurev.fluid.36.050802.122121>